Eur Biophys J (1999) 28: 357–368

ARTICLE

Toyoaki Matsuura · Sridhar Gorti · Toyoichi Tanaka
Yoshiaki Hara · Mototsugu Saishin

Determination of corneal gel dynamics

Received: 18 March 1998 / Revised version: 4 February 1999 / Accepted: 4 February 1999

Abstract From observations of the dynamics of light scattered by the cornea, intensity autocorrelation functions that revealed two independent diffusion coefficients, D (fast) = $2.4 \pm 0.2 \times 10^{-7}$ cm^2/s and D (slow) = $9.4 \pm 1.3 \times 10^{-9}$ cm^2/s, were obtained. The diffusion coefficients were found to be statistically independent of the position and depth on the lateral surface of the cornea from which the scattered light was sampled. The slow diffusion coefficients obtained from light sampled from within cross-sections of the cornea were, however, measurably different. Diffusion coefficients obtained independently from observations of the kinetics of corneal swelling for comparison were found to be several orders of magnitude greater than those obtained from light scattering. The large disparity in the diffusion coefficients obtained from the two independent methods invoked the possibility that the lamellar layers within the cornea behave as individual gel sheets. Irrespective of this additional hypothesis, divergent behavior in the measured total scattered light intensities and diffusion coefficients upon varying external conditions, such as temperature or pressure (stretching), was observed. Namely, a slowing down of the dynamic modes accompanied by increased "static" scattered light intensities was observed. Although the slowing down of the dynamic modes is possibly indicative of the reduced affinity of protein binding to the gel matrix that "softens" the gel, the divergent behavior in the scattered light intensities and diffusion coefficients is, however, more characteristic of a phase transition. In addition, the divergent behavior in the scattered light intensities and diffusion coefficients was reversible up to a critical temperature (~55 °C) or stretching (~16%).

Key words Cornea · Gel · Light scattering · Phase transition

T. Matsuura[1] · S. Gorti[2] · T. Tanaka (✉)
Department of Physics,
Center for Materials Science and Engineering,
and George R. Harrison Spectroscopy Laboratory,
Massachusetts Institute of Technology,
Cambridge, MA 02139, USA

Y. Hara · M. Saishin
Department of Ophthalmology,
Nara Medical University Kashihara-shi, Nara, Japan

Present addresses:
[1] Department of Ophthalmology,
Nara Medical University Kashihara-shi, Nara, Japan
[2] Laboratory for the Structure of Matter, Code 6030,
Naval Research Laboratory,
4555 Overlook Avenue, SW, Washington, DC 20375-5342, USA

Introduction

Significant progress in both theoretical and experimental investigations of complex polymer systems enables one to now predict unambiguously the physico-chemical properties of polymer networks or gels (Flory 1953; Tanaka et al. 1980). Gel networks are simply polymers cross-linked to create an enmeshed network within a liquid medium. The cross-linking of polymers gives rise to unique physical characteristics that are otherwise not exhibited by the polymers in solution alone. For example, gels maintain their shape and rigidity by "trapping" fluids within the network. The mean field theory of Flory-Huggins for polymer gels predicts that gel rigidity and the ability of a gel to retain fluids are dependent not only on the physico-chemical composition of the network, but also on the interaction between the network and the fluid medium. The physico-chemical composition of the network determines the extent of polymer-polymer interactions within the network for a given solvent condition (Flory 1953).

The Flory-Huggins theory also predicts the existence of phase transitions within gels (Tanaka et al. 1980): when the medium is a good solvent, the affinity for polymer-polymer interactions becomes small compared with polymer-solvent interactions, causing the polymers to expand and the gel matrix to swell. Conversely, when the fluid medium is a poor solvent, the affinity for polymer-polymer interactions becomes large and the polymers collapse onto themselves, causing the gel to shrink. As the solvent con-

ditions are varied gradually from a good solvent to a poor solvent, gels undergo a volume phase transition from a swollen phase to a shrunken phase (Tanaka et al. 1980). Several external conditions, such as temperature, pH, light, and pressure, can also induce either continuous or discontinuous reversible volume phase transitions in covalently or "permanently" cross-linked gels by affecting the affinity for polymer-polymer and/or polymer-solvent interactions (Tanaka et al. 1980; Li 1989; Mamada et al. 1990). By varying a combination of external conditions, phase diagrams could then be constructed for any gel.

The investigations of gel behavior initiated the hypothesis that the observed gel volume phase transition is analogous to the reversible gas-liquid phase transition. Knowledge of gas-liquid phase transitions dictates that gel volume phase transitions must also be accompanied by critical phenomena (Landau and Lifshitz 1990). Namely, a region within the volume phase diagram of a gel exists, wherein critical phenomena must be observed as conditions, such as gel density, temperature, pressure, etc., approach a critical point. The earliest indications of critical behavior in gels were from simple observations of gels becoming opaque, reversibly, at specific locations within the phase diagram. Unlike phase transitions that can be investigated simply by monitoring volume changes, experimental verification of critical phenomena, however, required the application of laser light scattering technologies. A critical juncture in the advancement of gel research was the realization that scattered light intensity fluctuations, arising from concentration or density fluctuations within gels, represented thermally excited acoustic or elastic vibrations of the gel matrix (phonons) that are rapidly dampened by frictional forces (Tanaka et al. 1973). Subsequent light scattering experiments were able to verify that: (1) the magnitude of scattered light intensity fluctuations were dependent upon the compressibility of the gel network, (2) the ratio of the elastic modulus and the frictional coefficient of the network in its fluid medium, or the effective "pore" size of the network, can be determined by the gel diffusion coefficients obtained from the decay times of the intensity correlation functions, and (3) as the gel approaches the critical point, critical phenomena can be evidenced in the form of divergent behavior in the observed scattered light intensities and the gel diffusion coefficients (Tanaka et al. 1980). Namely, the gel simultaneously becomes infinitely compressible as the pore size becomes infinitely large. Thus, the observed scattered light intensities should markedly increase while the diffusion coefficients diminish towards zero. Critical divergence has been shown to occur simultaneously as the gel approaches the critical point within the phase diagram and exhibits critical opacity (Tanaka et al. 1980).

Phase transitions and critical phenomena observed in synthetic polymer gels are considered to be characteristics universal to all gels. Regardless of their physico-chemical composition, all polymer networks should then exhibit phase transitions and critical phenomena under appropriate conditions. A simple confirmation of this assertion was demonstrated by inducing phase transitions in gels that were made up of cross-linked biopolymers (Amiya and Tanaka 1987). The "bio-gels" were formed from artificially cross-linked biopolymers, such as DNA, agarose, and gelatin. However, there have been no studies detailing the phase transitions and critical phenomena of gels formed in nature.

Consider the cornea, the outermost protective layer of tissue in the eye that is transparent to visible light. The cornea's structure, in brief, consists of several physiologically different layers (Maurice 1984). Its most voluminous component is the corneal stroma (~90%) which itself is also comprised of numerous sheets or layers of highly organized collagen fibrils, lamella (Maurice 1984). Within each layer, a cross-linked polymer matrix that fills the interfibrilar space surrounds the collagen fibrils. Externals to this complex gel matrix are cells scattered throughout (Scott and Haigh 1985). Within each lamellar layer, however, the collagen fibrils are unidirectionally aligned in regular anisotropic order. All layers are stacked one upon another in parallel with the lateral surface of the cornea; the collagen fibers also lie in parallel with respect to the corneal surface (Maurice 1984). Physical characteristics of the cornea have been well studied, in particular, using electron microscopy (Farrell and McCally 1976; Maurice 1984; Gisselberg et al. 1991) and small-angle static light scattering methodologies (Bettelheim and Vinciguerra 1969; Cejtlin et al. 1971; McCally and Farrell 1977). In investigations of the cornea, it had often been alluded to as a gel network; hence the application of light scattering methodologies for determining its structural properties (Bettelheim and Vinciguerra 1969). Essentially no investigations on the dynamics and phase equilibrium properties of the cornea, however, have been performed to verify indisputably that the cornea is indeed a gel network.

Some diseases affect changes in the highly complex structure of the cornea that induce opacification. In addition to diseases, corneal transparency is also impaired when abnormally high pressure is applied (Maurice 1984; Gisselberg et al. 1991), or after photorefractive keratectomy (Lohmann et al. 1992). Intraocular pressure in acute glaucoma, for example, can induce corneal opacity, which disappears immediately upon the pressure being alleviated (Waltman and Hart 1970). Also, in some cases, it has been reported that reversible cloudiness or haze was caused by photorefractive keratectomy (Lohmann et al. 1992). The reversible property of corneal gel opacities perceptibly demonstrates that the cornea may behave typically like a gel network, as its chemical make-up would indicate. If indeed the cornea were a gel network, well-established theories would predict that the cornea should exhibit phase transition and critical phenomena in response to varied external conditions. The present research thus places emphasis on measurements of scattered light intensities and dynamics from calf corneas, subjected to changes in the external conditions, to determine the existence of phase transitions and critical phenomena in the corneal gel.

Materials and methods

Experimental materials

Calf eyes were obtained freshly, within ~5 h, from a local slaughterhouse. The approximate age of the calves was 1 year. Immediately upon receipt, whole corneas from some of the calf eyes were excised in a nutrient mixture F-10 solution (GIBCO Laboratories). In some of our investigations, whole eyes from the slaughtered calves were also used shortly after being received and cleansed with F-10 solution.

Microscope laser light scattering spectroscopy

A schematic diagram of the MLLSS apparatus is illustrated in Fig. 1 (Nishio et al. 1983). The MLLSS design utilized focusing optics that allowed for light exiting a 30 mW He-Ne laser (632.8 nm wavelength) to be interfaced with a single mode optical fiber. The optical fiber serves as a light guide whose "output" end coupled to a micro-lens (Applied Fiber Optics) focused the laser light exiting the optical fiber within a specified region of the cornea that was resting at the focal plane of the microscope (Nikon). The basic components and configuration of the remainder of the MLLSS apparatus are:

1. A microscope objective that collects the scattered light that was magnified 32×.
2. A microscope eyepiece (Gamma Scientific) with an embedded optical fiber that collects scattered light within a ~1.92 μm^2 sampling area and guides the light to the photo multiplier tube (PMT: Thorn EMI); the latter converts and amplifies the incoming photons to an analog electric current.
3. An amplifier-discriminator (Pacific Instruments) converts the analog ac photo current into a digital transistor logic (TTL) pulse train.
4. A counter that measures the number of photon counts that are detected per second.
5. A correlator (Brookhaven Instruments) computes the intensity correlation function from the TTL pulse train.
6. A computer stores and analyzes the intensity correlation function of the scattered light, as well as the number of photon counts/second that were observed.

In the current configuration, the scattered light sampling volume detected by MLLSS was ~8 μm^3, determined by the magnification power (32×) and the depth of focus of the microscope objective (~4 µm; based on a numerical aperture of 0.40), and the core diameter of the optical fiber (50 µm) embedded within the eyepiece.

The distinguishing feature of MLLSS is the ability to select visually the portion of the magnified image that is transmitted to a photo multiplier tube. As in conventional dynamic light scattering spectroscopy, however, MLLSS measures the intensity correlation function, $C(\tau)$, from the observed time-dependent fluctuations in the intensity of

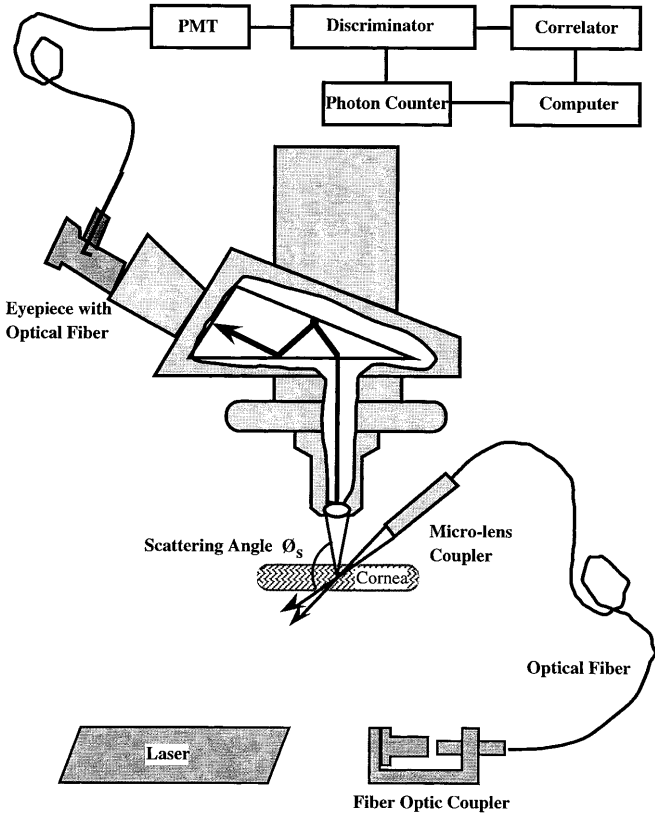

Fig. 1 A schematic of the technique of microscope laser light scattering spectroscopy (MLLSS)

light scattered by the cornea. The intensity correlation function is written as (Berne and Pecora 1976):

$$C(\tau) = \langle I(t)\, I(t+\tau)\rangle_t \quad (1)$$

where the angle brackets denote time (t) average, and $I(t)$ represents the intensity of scattered light. In our MLLSS investigations of the cornea, the time-dependent scattered light intensity fluctuations represent local dynamic swelling and shrinking of the corneal gel that give rise to local concentration or refractive index fluctuations. Moreover, an additional "stationary" component in the scattered light intensity due possible to permanent, static inhomogeneities within the cornea is also present. Thus the scattered light intensity can be considered to consist of both static, I_S, and dynamic components, $I_D(t)$ (Peetermans et al. 1986):

$$I(t) = I_S + I_D(t) \quad (2)$$

The observed fluctuations in intensity, $I(t)$, with time, is a measure of the fluctuations in the average magnitude of the Poynting vector, expressed in terms of the scattered electric field $E(t)$ as: $I(t) = E(t) \cdot E^*(t)$, according to Poynting's theorem. The intensity auto correlation function, $C(\tau)$, for a system containing immobile and mobile species, is rewritten in terms of the normalized electric field correlation function, $g(\tau)$, as follows (Berne and Pecora 1976):

$$g(\tau) = \langle E(t) \cdot E^*(t+\tau)\rangle / \langle E(t) \cdot E^*(t)\rangle \quad (3)$$

and (Peetermans et al. 1986):

$$C(\tau) = (I_S + I_D) + A\,\{I_D^2\, g^2(\tau) + 2 I_S\, I_D\, g(\tau)\} \quad (4)$$

where the quantity A accounts for both a finite sample time and a finite scattering angle. For the present set of conditions, we have experimentally determined A to be 0.8 by fitting intensity correlation function data obtained from a known standard using a simple exponential relaxation process for $g(\tau)$ [$g(\tau) = e^{-Dq^2\tau}$] and setting $I_S = 0$ in Eq. (4). Here D is the diffusion coefficient of the standard particle, q is the magnitude of the wave vector defined by the scattering angle θ and the wavelength λ of the laser:

$$q = \frac{4\pi n}{\lambda} \sin\frac{\theta}{2} \quad (5)$$

In the present experiments, q was approximately $2.44 \pm 0.03 \times 10^5$ cm^{-1}.

The light scattered intensity correlation functions obtained from the cornea exhibited non-exponential behavior. This non-exponential behavior can be represented by a distribution of exponentially relaxing processes for $g(\tau)$. For simplicity, two independent decay processes to describe the data, simply ascribed the subscripts f and s representing the "fast" and "slow" distributions of diffusion motions, respectively, were used. Hence the normalized electric field correlation function is assumed to decay as

$$g(\tau) = \frac{A_f}{A_s + A_f} e^{-D_f q^2 \tau} + \frac{A_s}{A_s + A_f} e^{-D_s q^2 \tau} \quad (6)$$

It is understood that fluctuations in the density (ϕ) of a gel network are governed by cooperative or collective diffusion motions (Tanaka et al. 1973):

$$\frac{\partial \phi}{\partial t} = D \nabla^2 \phi \quad \text{where } D \equiv \frac{(K + 4\mu/3)}{f} \quad (7)$$

is the collective diffusion coefficient of the gel, K and μ are the osmotic bulk modulus and the shear modulus of the network, respectively, and f is the friction between a unit cube of the gel network and fluid, when the fluid and network move with a unit relative velocity. Thus the correlation function of the density fluctuations, $\phi(t)$, for a particular wave vector is given by (Tanaka et al. 1973):

$$\langle \Delta\phi(t+\tau) \cdot \Delta\phi(t) \rangle_t = \langle \phi^2 \rangle \exp[-D q^2 \tau] \propto \frac{kT}{M} \exp[-D q^2 \tau] \quad (8)$$

where $M = K + 4\mu/3$ is the longitudinal modulus, and kT is thermal energy. For the case of two independent decay times (f = fast, and s = slow) assumed for the normalized electric field correlation functions, we assign the following density correlation function to describe such a process:

$$\langle \Delta\phi(t+\tau) \cdot \Delta\phi(t) \rangle_t = \frac{kT}{M_f} \exp[-D_f q^2 \tau] + \frac{kT}{M_s} \exp[-D_s q^2 \tau] \quad (9)$$

where the M's are longitudinal moduli corresponding to the two different longitudinal diffusion motions. The correlation function $g(\tau)$ in Eq. (6) is directly proportional to the density correlation function in Eq. (9) (Tanaka et al. 1973). As a direct consequence the observed diffusion coefficients D [Eqs. (7) and (9)], and scattered light intensities, in particular I_D [Eq. (4)], become divergent as the gel approaches a critical transition. Namely, the gel becomes infinitely compressible and concentration fluctuations become slowed down as a critical transition is approached. (Note: the osmotic compressibility of a gel is inversely proportional to the bulk modulus K). The magnitude of I_D is directly proportional to the osmotic compressibility ($1/M$). The parameters A_f and A_s in Eq. (4) represent the relative contributions of each modulus to the overall gel compressibility. All intensity correlation function data were analyzed using Eqs. (4)–(6).

MLLSS of the cornea

Using either the excised corneas or the whole eye, the following experiments were performed:

1. We first determined the light scattering dynamics of the cornea with respect to location and depth at which the scattered light was sampled from the anterior surface. At a given position on the lateral surface, the focal depth at which the scattered light was sampled varied from approximately 0.1 mm to 0.9 mm.
2. Cross-sections of corneas were used to determine the dependence of the anisotropic lamellar layer ordering on the dynamics observed by MLLSS.
3. The effects of increased temperatures on the corneal dynamics were also investigated on excised whole corneas immersed in silicone, within a sealed glass cell. The temperature of the cell was adjusted by circulating water from a controlled temperature bath.
4. Whole corneas further excised with a trepan into a rectangular shape of 2 mm×10 mm were used to determine the dependence of MLLSS data upon stretching. The cornea was stretched by placing the two ends of a rectangular shaped piece of an excised cornea between glass plates, where both ends were held fixed in a vice-like device that could translate along the lengthwise axis of the cornea. During the course of stretching, the cornea was immersed in silicone not only to prevent it from drying or swelling, but also to limit specular reflections.
5. In situ MLLSS experiments to demonstrate the effects of increased intraocular pressures on corneal dynamics were also performed. Whole eyes immersed in silicone oil were subjected to an increase in internal pressure. The internal pressure of the eye was regulated by the use of a manometer system. That is, a syringe attached to a graduated cylinder by a rubber tube is directly injected into the anterior chamber of the calf eye. Internal pressure within the calf eye was controlled hydrostatically by varying the height of the water level between the calf eye and water within a graduated cylinder.

All MLLSS data were collected within 8 h of receipt of calf eyes from the slaughterhouse. Unless otherwise indicated, all MLLSS data were also obtained using a scattering angle of 135° at a temperature of 23°C and a focal depth of approximately 0.1–0.2 mm within the cornea, and the average thickness of the calf eye corneas used was ~1.0±0.1 mm. Furthermore, all data regarding the above experiments were repeated a minimum of two times.

Thickness measurements of the cornea

Some whole corneas were further excised with a trepan into a rectangular shape of 2 mm×10 mm. These excised corneas were placed in distilled de-ionized water and were allowed to reach their equilibrium shape. The thickness of the cornea was recorded using a microscope with an ocular scale, in time, as the gel became swollen. Time zero is established the instant the excised cornea was immersed within the distilled de-ionized water.

Results

Intensity correlation functions were collected using several different sampling times: 4, 10, 20 and 40 μs. All correlation functions obtained form these various sampling times appeared to be multi-exponential in form. The error in both the fast and slow diffusion coefficients obtained from the first three sampling times was, on the average, less than 12%. Both the "fast" and "slow" diffusion coefficient data obtained from a sampling time of 40 μs were, however, systematically lower by approximately a factor of two. Analyses of data upon truncation also yielded results that differed systematically. The magnitude of the difference was dependent on the time window used. This behavior is indeed expected of multi-exponential functions. Hence the values obtained for both the fast and slow diffusion coefficients using Eqs. (4)–(6) are apparent values that depend both on the time window and sampling time used. Despite the limitations imposed, both the fast and slow diffusion coefficient data exhibited statistically significant trends that can be subjected to various forms of interpretation.

Figure 2 exhibits a correlation function obtained by MLLSS from observations of light backscattered at the anterior surface of the cornea from an approximate depth of ~0.1 mm, observed at a scattering angle of 135° and at a temperature of 23°C. From non-linear least squares fit to the data using Eqs. (4)–(6) (the solid line in Fig. 2), the essential parameters for the diffusion constants D_f = 2.1×10^{-7} cm^2/s and D_s = 9.6×10^{-9} cm^2/s that represents the two apparent, collective diffusion motions of the corneal gel, designated as fast and slow motions, respectively, were derived. Other significant parameters of the computer generated fit include the relative contributions of the fast and slow components to the overall dynamic scattered light intensity I_D, designated as $\%A_f$ and $\%A_s$, respectively, where $\%A_f = 100\times A_f/(A_f+A_s)$. The static $\%I_S$ and dynamic $\%I_D$ components of scattered light intensities, where $\%I_D = 100\times I_D/(I_S+I_D)$, to the total scattered light intensity I_t observed at a particular wave vector, were also determined. For the data shown in Fig. 2, $\%A_f \approx 40$ and $\%I_D \approx 30$.

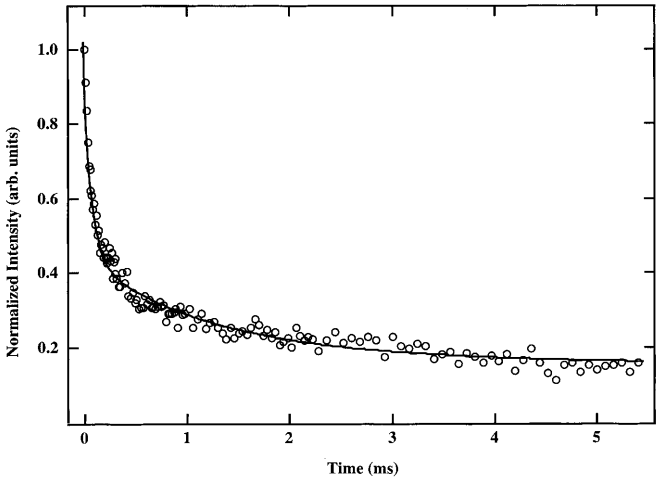

Fig. 2 A single correlation function (○) as determined by the technique of MLLSS from light scattered by the calf cornea. The data were collected using a scattered light collection angle of 135° and at a temperature of 23°C. The *solid line* represents a computer-generated fit to the data using Eqs. (4)–(6) of the text. The results of the fit yielded for the "fast" mode D_f = 2.1×10^{-7} cm^2/s, the "slow" mode D_s = 9.6×10^{-9} cm^2/s, and $\%A_f$ = 40 which represents an approximate value for the relative concentration of the fast scatterer present within the cornea

Dependence on location and depth of measurement from the anterior surface

Scattered light from several positions on the anterior surface of excised corneas was sampled at different depths ranging from 0.1 to 0.9 mm, with a scattering angle of 135° and at a temperature of 23°C. The distances between the relative positions sampled on the anterior surface of each cornea, schematically represented in Fig. 3a, were ~1 cm apart. Figure 3b shows the dependence of the averaged diffusion coefficients $\bar{D}_f$ and $\bar{D}_s$ obtained from sampling scattered light at several different depths, with respect to the seven relative positions on the lateral surface of the cornea. As observed, neither $\bar{D}_f$ nor $\bar{D}_s$ exhibit statistically significant differences either with respect to position on the anterior surface of the cornea or the depth at which scattered light was sampled. The cumulative or combined averages of $\langle\bar{D}_f\rangle$ and $\langle\bar{D}_s\rangle$ for all values presented in Fig. 3b are $2.4\pm0.2\times10^{-7}$ cm^2/s and $9.4\pm1.3\times10^{-9}$ cm^2/s, respectively. In addition, the combined averages of the relative contribution of fast scatterer to the dynamic component of scattered light I_D for all data was $\langle\%A_f\rangle \approx 40\pm5$, and the overall contribution of stationary sactterers to the total scattered light intensities was $\langle\%I_D\rangle \approx 31\pm4$.

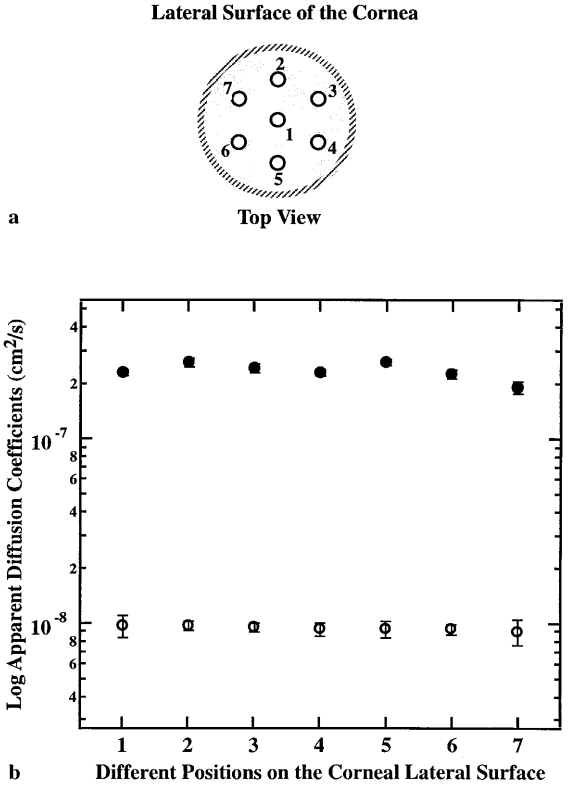

Fig. 3 **a** A schematic of the lateral surface of a calf cornea with *numbered circles* representing the seven different locations where the scattered light from different depths within the cornea was sampled. **b** The averages of the diffusion coefficient data D_f (●) and D_s (○) obtained at several depths at each location from the lateral surface of different corneas. The diffusion coefficient data were collected using a scattered light collection angle of 135° and at a temperature of 23 °C

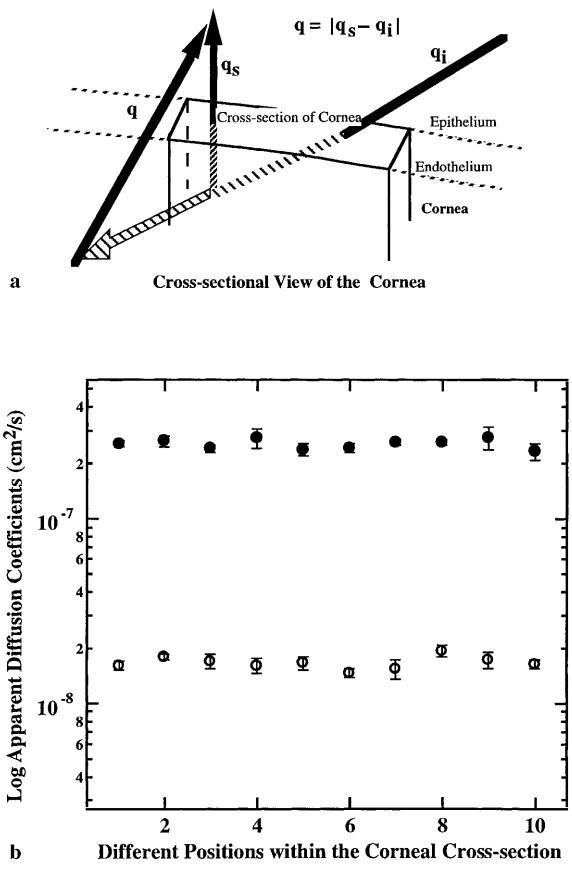

Fig. 4 **a** A schematic of a cross-sectioned calf cornea to determine the dependence of the collagen fibrils, ordering on the observed light scattering dynamics. **b** The averages of the diffusion coefficient data D_f (●) and D_s (○) obtained at several locations on different cross-sectioned corneas. At a temperature of 23 °C, the diffusion coefficient data were collected using a scattered light collection angle of 135°

Dependence of fibril orientation within cross-sections of corneas

The dependence of the anisotropic ordering of collagen fibrils within the independent lamellar layers on the observed light scattering dynamics was also investigated. In these studies, scattered light was collected form within cross-sections of corneas placed on the microscope stage, as shown schematically in Fig. 4a. Scattered light was collected at 10 different locations for several different corneal cross-sections, at approximately equidistant spacing (~30 µm intervals) leading away from the anterior surface of the cornea, at scattering angle of 135° and at a temperature of 23 °C. Figure 4b shows the dependence on the averaged diffusion coefficients $\bar{D}_f$ and $\bar{D}_s$ obtained from sampling scattered light at several different positions on the corneal cross-sections at an approximate depth of 0.1 mm. As evidenced, neither $\bar{D}_f$ nor $\bar{D}_s$ exhibit statistically significant difference with respect to position on the corneal cross-section at which scattered light was sampled. The cumulative or combined averages of $\langle\bar{D}_f\rangle$ and $\langle\bar{D}_s\rangle$ for all values represented in Fig. 4b are $2.6\pm0.3\times10^{-7}$ cm^2/s and $20\pm3\times10^{-9}$ cm^2/s, respectively. The cumulative average of the relative contribution of the fast scatterer for all data was $\langle\%A_f\rangle \approx 30\pm8$, and the overall contribution of stationary scatterers to the total scattered light intensities was $\langle\%I_D\rangle \approx 36\pm5$.

Table 1 Summary of light scattering corneal dynamics

Location	Average $\langle\bar{D}_f\rangle$ (cm^2/s)	Average $\langle\bar{D}_s\rangle$ (cm^2/s)	$\langle\%A_f\rangle$	$\langle\%I_D\rangle$	$\langle\%I_S\rangle$
Surface of the cornea	$2.4\pm0.2\times10^{-7}$	$9.4\pm1.3\times10^{-9}$	40±2	31±4	69±8
Within the corneal cross-section	$2.6\pm0.3\times10^{-7}$	$20\pm3\times10^{-9}$	30±8	36±5	64±9

In Table 1, we summarize the results of our investigations regarding the dependence of the observed dynamics on the position and depth within the cornea, as well as dependence on the orientation of collagen fibrils within the corneal cross-sections. As evidenced by the data, only the averaged difffusion coefficient $\langle\bar{D}_s\rangle$ exhibits a measurable difference.

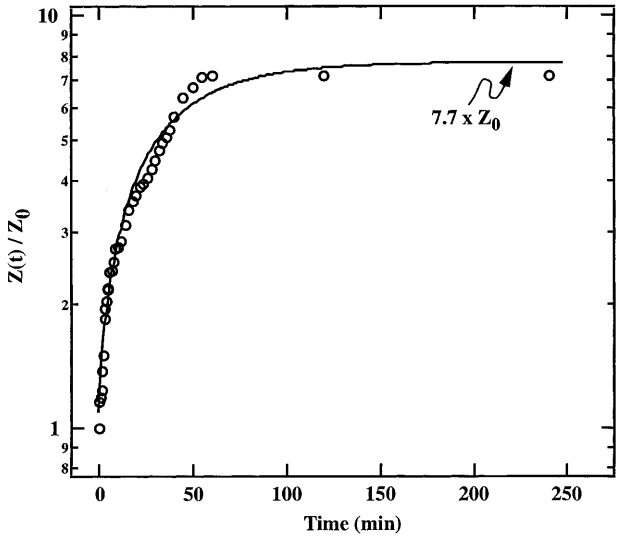

Fig. 5 Measurements in the change in the thickness $Z(t)$ of a 2 mm wide×10 mm long excised piece of cornea (○) as it expands from a collapsed state to a swollen state, with time, in the presence of water at 23 °C is shown as a ratio $Z(t)/Z_0$, where Z_0 is the initial thickness of the cornea. The *solid line* represents computer-generated fit to the data using Eq. (10). The relaxation time obtained for 7.7 times the initial thickness swelling of the cornea was τ_r = 40 min

Kinetics of corneal swelling

An alternate means for determining gel diffusion coefficients can be accomplished by observations of the rate at which a gel volume changes when subjected to an abrupt change in the external conditions. In this particular case, the initial equilibrium state of a gel, where the condition of zero osmotic pressure applies, is abruptly altered by immersion of the corneal gel into distilled deionized water, at 23 °C. If this perturbation is sufficiently small, the kinetics of the subsequent relaxation process (volume change) as the corneal gel tends towards a new equilibrium state will simply be exponential in form. Figure 5 shows the rate at which the ratio of the cross-sectional thickness of an excised corneal gel with respect to its initial thickness expands, in time, as it "relaxes" towards the new equilibrium-state. As the data are sigmoidal in form, the relaxation process can be represented by (Tanaka and Filmore 1979):

$$\frac{Z(t)}{Z_0} \approx a - b\exp(-t/\tau_r) \qquad (10)$$

where Z_0 is the initial thickness of the cornea, τ_r is the observed relaxation time for the thickness change, and a and b are constants whose magnitude is dependent on the gel dimensions. Because the gel is undergoing a change in volume, the rate limiting step that determines the characteristic relaxation times for swelling is considered to be the diffusion coefficient of the gel (Tanaka and Filmore 1979). For corneal swelling shown in Fig. 5, the relaxation time τ_r can be expressed as (Tanaka and Filmore 1979):

$$\tau_r \approx Z^2/4D_r \qquad (11)$$

Table 2 Light scattering dynamics of swollen corneas

Swelling ratio	Calculated τ_r	D_r calculated	Measured D_f and D_s
Not swollen, normal	–	–	$D_f = 2.1\times10^{-7}$ cm^2/s $D_s = 9.2\times10^{-9}$ cm^2/s
Swollen cornea	τ_r = 40 min	$D_r = 1.0\times10^{-4}$ cm^2/s	$D_f = 1.0\times10^{-7}$ cm^2/s $D_s = 5.6\times10^{-9}$ cm^2/s

where Z is the final thickness and D_r is the diffusion coefficient of the corneal gel as obtained from the relaxation measurement. From observations of swelling corneal gels and subsequent analysis of all temporal data using Eq. (10) (solid curve), we obtained $\tau_r \approx 40\pm5$ min and the final thickness (Z) of the swollen cornea was ~7.7 times its initial thickness, $Z_0 \approx 1.0$ mm. Substituting these values into Eq. (11) yields $D_r \approx 1\times10^{-4}$ cm^2/s, that is ~5 orders of magnitude greater than the gel diffusion coefficients $D_s \approx 6\times10^{-9}$ cm^2/s that were measured by MLLSS from the anterior surface of the same cornea at 8 times the swollen ratio and 23 °C (Table 2).

Effect of temperature on corneal dynamics

Scattered light was sampled at a depth of ~0.1 mm from the anterior surface of excised whole corneas at a scattering angle of 135°. Figure 6a displays the averaged fast and slow diffusion coefficients $\langle D_f\rangle$ and $\langle D_s\rangle$ obtained from three different corneas in the temperature range between 5 and 65 °C. As shown, both $\langle D_f\rangle$ and $\langle D_s\rangle$ increased along with the temperature up to 35 °C and then began to decrease and diminish at about 55–65 °C. The initial rise, up until 35 °C, in the values of both $\langle D_f\rangle$ and $\langle D_s\rangle$ reflects the decrease in the frictional coefficient f due to changes in the viscosity of water with respect to temperature. Figure 6a also contains values calculated for fast and slow diffusion coefficients, where only the temperature and corresponding values for viscosity, determined by using Cragoe's equation (Lange's Handbook of Chemistry 1985), were varied. Beyond 35 °C both $\langle D_f\rangle$ and $\langle D_s\rangle$ began to decrease with increasing temperatures.

The observed decrease in $\langle D_f\rangle$ and $\langle D_s\rangle$ with respect to increasing temperatures was also accompanied by a divergent behavior in the measured scattering intensity. Figure 6b displays the total intensity of light I_t scattered by the cornea at a scattering angle of 135° with respect to increasing temperatures. In the temperature range of 5–35 °C, I_t is essentially constant. As the temperature exceeds 35 °C, I_t increases dramatically and the cornea exhibits "cloudiness."

In instances where the temperature was reversed upon reaching ~55 °C, the divergent behavior observed between the measured diffusion coefficients and static scattered light intensities was reversible (see Fig. 6). Namely, both the observed diffusion coefficients and scattered light intensities recovered to their original val-

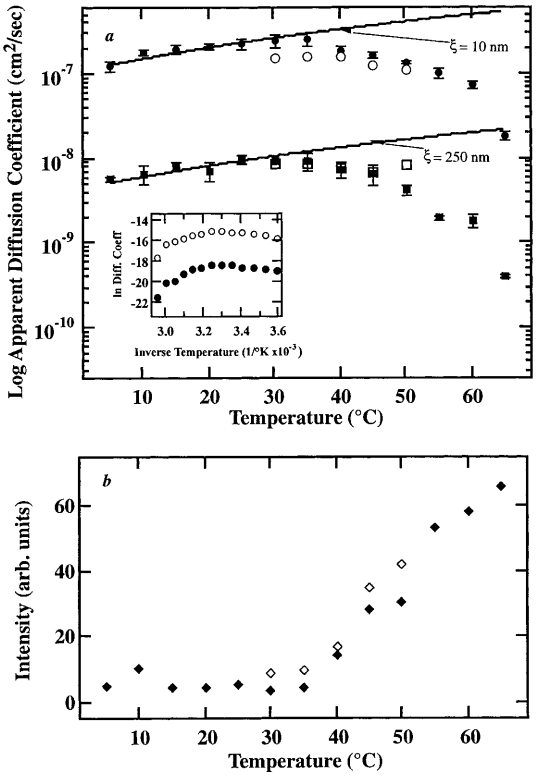

Fig. 6 **a** The effect of increased temperatures in range of 5–65 °C on the observed diffusion coefficients D_f (●) and D_s (■) are shown on a logarithmic scale. The *open circles* and *squares* represent the measured D_f and D_s, respectively, as the temperature was reversed upon reaching 55 °C. The *solid lines* represent expected values for D_f and D_s calculated using Eq. (12), where the changes in the viscosity were corrected using Cragoe's equation (Lange's Handbook of Chemistry 1985). As observed, the data are initially in good agreement with calculated values up to a temperature of 35 °C. Beyond 35 °C, both the observed diffusions coefficients D_f and D_s dramatically deviate from the expected values. The *inset* in **a** is an Arrhenius plot exhibited as the natural logarithm of the diffusion coefficients as a function of inverse temperature (K). **b** The dependence of the total scattered light intensity (◆) observed at the lateral surface of the cornea at a scattering angle of 135° with respect to increasing temperatures. As the corneal gel approaches the critical temperature, the observed scattered light intensities increase dramatically. The intensity (◇) also diminishes to its original value as the temperature is reversed upon reaching 55 °C

ues when the temperature was reversed upon reaching ~55 °C. Recovery of diffusion coefficients and scattered light intensities was, however, not observed with the reversal of temperature upon reaching ~65 °C (data not shown).

Dependence of corneal dynamics upon stretching

Intensity correlation functions were calculated from scattered light sampled at a depth of ~0.1 mm from the anterior surface, a scattering angle of 135° and a temperature of ~23 °C. The intensity correlation functions showed a dramatic change as stretching was imposed upon the corneas (Fig. 7). The collective diffusion coefficients D_f and D_s calculated from the intensity correlation functions, using Eqs. (4)–(6), decreased as the cornea became elongated or stretched, and diminished as the imposed extension of the cornea reached a maximum of 20% (Fig. 8a). The stretching percent is defined as 100× (final length − initial length)/initial length. The cornea became opaque as a threshold for stretching was approached in the range of 16–20% stretching.

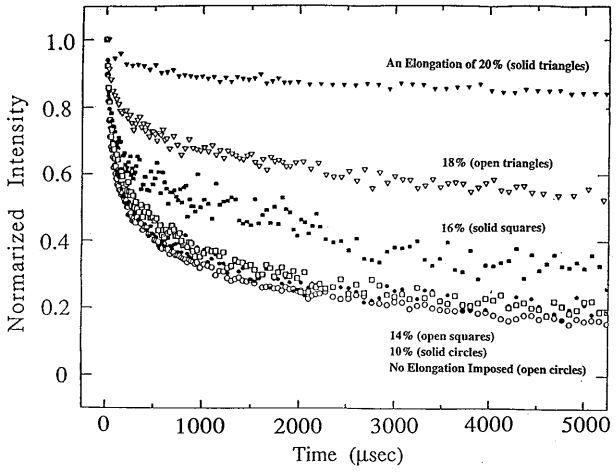

Fig. 7 The effects of increased stretching on the intensity correlation functions obtained from light scattered at the lateral surface. As evidenced, the "shape" of the correlation functions becomes "flattened" as the stretching approaches 16–20%

Parallel to the diminishment of the diffusion coefficients, the measured intensity I_t observed at a scattering angle of 135° increased and appeared to diverge as the stretching approached the critical threshold (Fig. 8b). The changes in I_t can be attributed to the increased compressibility of the corneal gel ($1/M_s$) as it approached the critical point of stretching. The divergent behavior in the observed diffusion coefficients and total scattered light intensities is indicative of the occurrence of a phase transition upon corneal stretching. These changes were reversible up to an imposed stretching of 15%.

As a simple means for demonstrating that a reversible stretching phase transition could cause corneal opacity in acute glaucoma, we observed the behavior of intensity correlation functions obtained from light scattered by in situ calf cornea upon increased intraocular pressures (IOPs). Here, only one pressure level was investigated to determine the effects of IOP on the corneal dynamics. Figure 9 displays the intensity correlation functions of the cornea under "normal" IOP, as well as when IOP was increased and subsequently alleviated. Upon raising the water level within the manometer system to a height of 50 mm (~35 mmHg) above the cow eye level, the increased internal pressure had "flattened" the intensity correlation function and the cornea appeared cloudy (Fig. 9). Upon removal of the excessive IOP, the correlation function regained its "sharp" decay and the cornea had cleared.

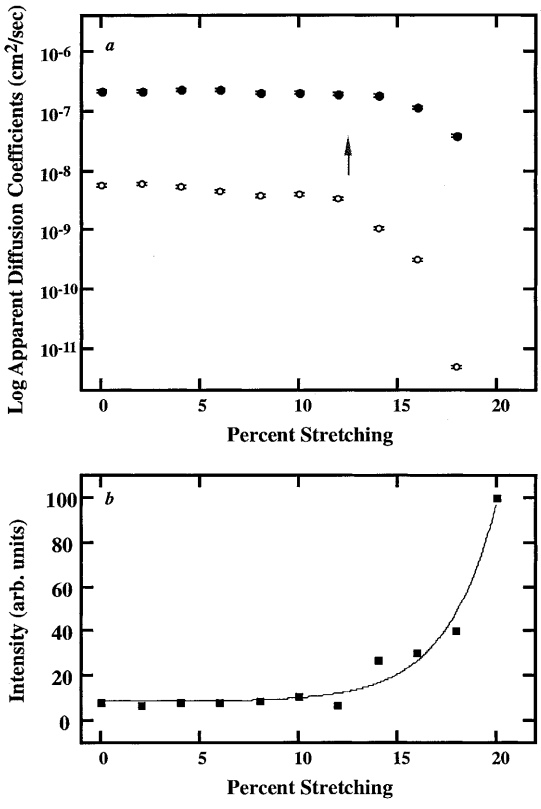

Fig. 8 **a** Diffusion coefficient data obtained as a lengthwise uniaxial stretching was imposed on the cornea are shown on a logarithmic scale. As evidenced, the observed diffusion coefficients D_f (●) and D_s (○) both slow down appreciably and diminish as the corneal gel approaches a critical stretching value between 16% and 20%. Also shown in **a** is the location where the observed ξ_s becomes larger than the wavelength of visible light (*arrow*). **b** Concurrent with the decrease in the observed diffusion coefficients, the total scattered light intensity (■) is also observed to increase dramatically

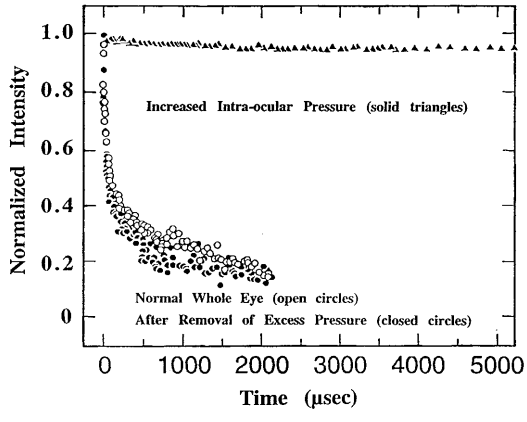

Fig. 9 The effects of increased intraocular pressure (IOP) on the observed back-scattered light intensity correlation functions. The initial "shape" of the correlation function becomes "flattened" as the IOP of the whole eye is increased by the injection of 50 ml of water. When the excessive IOP is removed, the correlation function essentially returns to its original "shape"

Discussion

The cornea is a very dense matrix of collagen fibrils whose transparency, as first demonstrated theoretically by Benedek (1971), is maintained not because of regular long-range ordering, but because spatial fluctuations in the number density of fibrils are small compared to unity. Simply put, the distance between collagen fibrils within the lamellar layers need only the shorter than the typical wavelength of light for the cornea to be transparent. Light can, however, be scattered by the collagen fibrils when their positions are randomly displaced, in time, due to thermal motions (Feuk 1970). Light can also be scattered by large "superstructures" or cells that are present throughout that stroma, which have an approximate size in the range of 1–20 μm (Kikkawa 1960; Bettelheim and Vinciguerra 1969; Maurice 1984). Stromal cells, primarily keratocytes, have dimensions of ~20 μm (Maurice 1984). The possibility that the superstructures are "wavy" lamellae that form in the absence of "normal" IOP was also proposed (McCalley and Farrell 1977).

In the time scale τ used to calculate the intensity correlation functions $C(\tau)$ from observations of light scattered from within the cornea, neither the motions of keratocytes nor the "wavy" lamellae of the approximate size ranging from 1000 nm to 20 000 nm would be correlated. Hence, light scattered by either the stromal cells or the wavy lamellae would contribute to the static component (I_S) of the overall scattered light (I_t) and not its dynamic component (I_D), as defined by Eq. (2). For simplicity, the dynamic component of the scattered light was assumed to be composed of two independent and uncorrelated diffusion processes characterizing local density fluctuations within the cornea. Under the assumptions invoked, preliminary analyses of light scattered by the stroma revealed several important characteristics, such as: (1) the total intensity of light scattered by the stroma I_t is composed of dynamic I_D (~30%) and static I_S (~70%) components and (2) the dynamic component of scattered light I_D is in itself composed of two independent longitudinal diffusion processes that were simply assigned as "fast" and "slow." The fast longitudinal diffusion motion contributes ~12% and the "slow" longitudinal diffusion motion ~18% of the total scattered light intensity I_t.

Time-dependent density fluctuations in synthetic gels arise as a result of thermally excited longitudinal and transverse vibration modes that are quickly dampened by viscous forces. The longitudinal mode vibrations are characterized by the collective diffusion coefficient D. (Note: the existence of transverse mode vibrations has yet to be verified experimentally.) The assumption that time-dependent density fluctuations in the cornea gel represents two independent diffusion motions arising from two independent longitudinal modes precedes any exact theory. For example, any number of exponential functions, beyond two, could be used to describe the data. For practical considerations, the bi-exponential form for the electric field correlation function $g(\tau)$ was employed, which well-fitted all

the observed intensity correlation functions, yielding meaningful and consistent results. Hence, higher order exponential forms were not used. Nevertheless, the actual intensity correlation functions may contain a broad distribution of relaxation times. To determine this distribution, however, the signal-to-noise ratio of the intensity correlation functions must be significantly improved before other numerical methods could be implemented to analyze the data. Under the assumptions invoked, however, an appreciable change in the observed diffusion coefficients with respect to the depth and location at which scattered light is collected from the anterior surface of the cornea and corneal cross-sections is not expected. The difference observed in the present study may be related to poor sample preparation, where corneas possibly became partially swollen upon excision within a nutrient bath.

In polymer gel theories, a simple relationship correlating the observed collective diffusion coefficient with the "pore" size of a network exists. Namely, the Kawasaki-Ferrell relation, the Stokes-Einstein equivalent for the collective diffusion coefficient of gels, can be used to determine the "pore" size of the collagen network (de Gennes 1979):

$$D(T) = \frac{kT}{6\pi\,\eta(T)\,\xi} \tag{12}$$

where $\eta(T)$ is the temperature dependent viscosity of the "trapped" fluid. The parameter ξ is the correlation length of the concentration fluctuations in the network, which in theory represents conceptually either the average distance between neighboring cross-links in the network (pore size) or the size of segments constituting the network polymers (Tanaka et al. 1973; Tanaka 1978). In practice, the spatial arrangements of randomly formed gel networks are not well known to offer any direct comparison with the values calculated for the parameter ξ. The spatial arrangement of collagen fibrils within the cornea is, however, well understood (Farrell and McCally 1976; Maurice 1984; Gisselberg et al. 1991). Hence, it is of interest to compare the known spatial arrangement of collagen fibrils within the cornea with the measured gel diffusion coefficients. Using Eq. (12), the parameter ξ was calculated for the above-cited experimental values and we obtained $\xi_f \approx 12$ nm and $\xi_s \approx 250$ nm for the fast and slow diffusion constants, respectively. Table 3 shows the different values calculated for ξ based on diffusion coefficients obtained from scattered light sampled near the anterior surface of the cornea as well as within corneal cross-sections. The values obtained for ξ shown in Table 3 do not correspond directly to any of the known dimensions of the corneal gel network. That is, it is well known that the average diameter of the collagen fibrils within lamellae is approximately 25 nm and the mean interfibrillar spacing is approximately 60 nm (Meek et al. 1991). A recent study evaluating the collagen fibril structure and organization within the bovine cornea by spatial Fourier analyses of electron micrographs had, however, reported the presence of Fourier components in the 200–1100 nm range (Gisselberg et al. 1991). Although Eq. (12) may not predict the actual structure of the collagen network, the parameter ξ may be useful for determining the swollen state of the corneas and can have practical applications in the clinical determination of the onset of corneal opacification or haze (see below).

Table 3 Pore size of the corneal gel

Location sampled	Combined averages of $\langle D_f \rangle$ (cm^2/s) and $\langle \xi_f \rangle$	Combined averages $\langle D_s \rangle$ (cm^2/s) $\langle \xi_s \rangle$
Surface of the cornea	$2.35 \pm 0.24 \times 10^{-7}$ $\langle \xi_f \rangle = 10 \pm 1$ nm	$9.43 \pm 1.3 \times 10^{-9}$ $\langle \xi_s \rangle = 260 \pm 31$ nm
Within the corneal cross-section	$2.55 \pm 0.29 \times 10^{-7}$ $\langle \xi_f \rangle = 9.6 \pm 1$ nm	$19.6 \pm 2.6 \times 10^{-9}$ $\langle \xi_s \rangle = 125 \pm 16$ nm

The collective diffusion process of a gel network not only determines the concentration fluctuations in the gel, but also the kinetics of macroscopic swelling and shrinking (Tanaka and Fillmore 1979; Hecht and Geissler 1980). Namely, swelling kinetics of the cornea should be governed by the diffusion of the corneal gel network and not by the diffusion of water. In order to provide a better understanding of the network structure, an independent measure of the corneal gel diffusion coefficient was thus considered. The diffusion coefficients obtained from observations of changes in the thickness of the cornea upon swelling, however, were approximately 3–5 orders of magnitude greater than those obtained from light scattering measurements of the same sample. From the outset, calculations of the collective diffusion coefficients from swelling kinetics assumed that the characteristic time of swelling corresponds to the thickness swelling of the whole cornea, whose initial thickness Z_0 was ~1.0 mm. The overestimation of D_r suggests that the observed kinetics of corneal swelling occurred far too rapidly for a cornea of this thickness and known collective diffusion coefficient. Since the measurements of both τ_r and D are relatively unambiguous, it is then possible to hypothesize that the inherent layered structure of the corneal stroma gives rise to the over estimation of D_r. For example, consider that each lamellar sheet of thickness Z_0^* within the stroma behaves as an individual gel. Calculating Z_0^*, instead of D_r, using Eq. (11) and the measured values for D and τ_r should then yield the average thickness of a lamellar layer (1–2 µm) within the corneal stroma. Using $\tau_r \approx 40$ min (relaxation time for a swelling of ~7.7 times) and $D_s \approx 7 \times 10^{-9}$ cm^2/s, we obtained $Z_0^* \approx 9$–11 µm. This value for Z_0^* is in much better agreement (within fivefold). The fivefold error is, however, still substantial and may be accounted for when better procedures for determining the swelling kinetics of individual lamellar layers are followed, a subject of future investigations.

The dynamics of corneal gels were also investigated with respect to externally increased temperatures or stretching. Under conditions of increased temperatures or stretching, the cornea approached a critical point where it became opaque. Critical opalescence occurs as a result of large-scale temporal fluctuations in the local densities of the collagen gel, where regions of high and low collagen

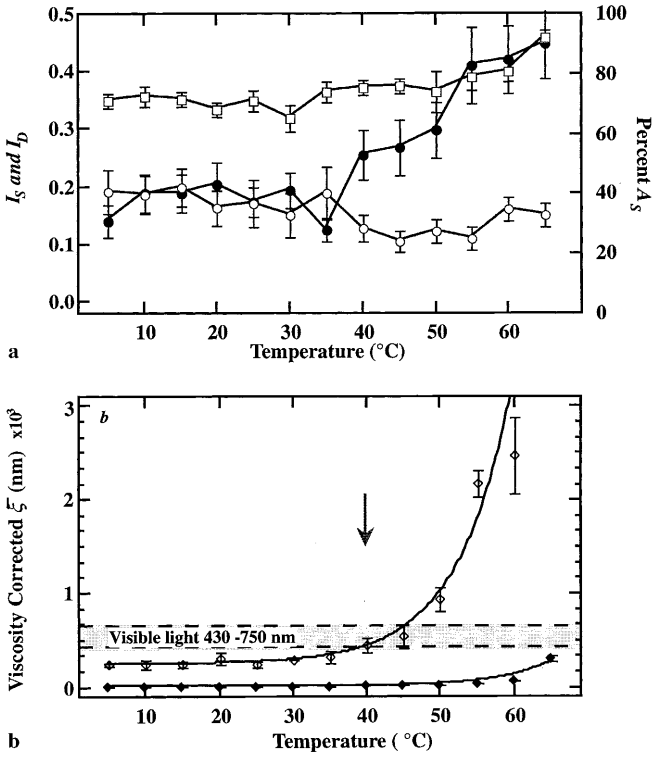

Fig. 10 **a** The static I_S (○) and dynamic I_D (●) component contributions to the total scattered light intensity I_t, obtained from fits to correlation functions using Eqs. (4)–(6), as a function of increasing temperature. The corresponding contribution of the "slow" scatterer $\%A_s$ (□) to the overall increase in I_D is also shown. The dramatic increase in I_D is indicative of increased amplitudes of local density fluctuations that usually accompany a phase transition. **b** The effective pore sizes ξ_f (◆) and ξ_s (◇) calculated using Eq. (12) from the observed diffusion coefficients D_f and D_s, respectively. At the outset, both ξ_f and ξ_s are relatively small upon comparison with the wavelength of visible light λ (magnitude is depicted by the *horizontal lines*). The magnitude of ξ_s, however, becomes not only comparable to λ but also much larger than λ beyond ~50 °C. The *solid lines* are visual guides for observing the data, and the *arrow* indicates the region of temperature where the cornea became visibly opaque

densities form. Thus, as a phase transition is approached, the magnitude of intensity fluctuations increased while they become slowed down. This behavior was readily evidenced by a divergent behavior in the observed scattered light intensities (I_t) and diffusion coefficients (D_f and D_s). Moreover, the dramatic increase in the observed scattered light intensities I_t is associated directly with an increase in the dynamic component of the scattered light I_D rather than the static component I_S (Fig. 10a). The primary contributor to the increase in I_D is the "slow" mode, where an increase in $\%A_s$ is also observed as the temperature was increased (Fig. 10a). This behavior is indicative of a gel undergoing a phase transition. The phase transition behavior of the cornea may well account for reported formations of fibril "lakes" within the lamellar layers (Cejtlin et al. 1971; Meek et al. 1991).

It is now important to note that reversible trends in the apparent diffusion coefficients may also arise as the affinity for protein binding to the gel "backbone" varies reversibly with temperature according to Arrhenius's law. That is, the affinity for protein binding to the gel backbone, by definition, is determined by the equilibrium constant K_D given by Arrhenius's law as: $K_D = K_0 \exp(-H/kT)$, where K_0 is a pre-exponential constant and H is the activation energy. As the temperature is increased, the affinity for protein binding to the gel matrix is reduced and the gel becomes soft, as fewer cross-links are present within the gel system. A direct consequence of fewer cross-links being present is a subsequent increase in ξ, the correlation length of the concentration fluctuations in the network. Hence the apparent diffusion coefficient(s) of the gel matrix is expected to decrease with increasing temperatures, as $D \propto K_D$. If the assumption were valid, then an Arrhenius plot of the logarithm of D versus $1/T$ should yield a linear relation, with a negative slope (see inset in Fig. 6a). The advancement of the protein binding affinity hypothesis in describing the observed trends in the diffusion coefficients at increased temperatures is, however, obviated for the following reasons:

1. The observed changes in diffusion coefficients are well-described by changes in the viscosity of the gel fluid, up to 35 °C (see Fig. 6a).
2. The Arrhenius plot of the logarithm of D versus $1/T$ is non-linear and non-negative, particularly beyond 35 °C (see Fig. 6a).
3. The hypothesis cannot realistically account for the divergent behavior in scattered light intensities, at increased temperatures.

Although the protein binding affinity hypothesis is not considered to be applicable in describing the observed data, phase diagrams for the cornea should be constructed to prove conclusively that phase transitions occur in corneal gels.

Regardless of the hypothesis invoked to describe the observed trends in the diffusion coefficients, the pore size of the stromal gel as the temperature is increased becomes much larger than the wavelength of light. Figure 10b displays the viscosity corrected pore size as a function of increased temperatures. As evidenced, the pore size ξ_s becomes comparable to the wavelength of visible light λ in the vicinity of 40 °C and larger than λ beyond 45 °C, where corneal opacity occurs.

The cornea also became opaque as the critical threshold for stretching was approached in the range of 16–20% stretching, where the pore size ξ_s also becomes much larger than the wavelength of visible light λ (data not shown). Divergent behavior in the observed diffusion coefficients and total scattered light intensities had also occurred (Fig. 8), which is indicative of the occurrence of a phase transition upon corneal stretching. The phase transition behavior of the corneal gel is completely reversible up to 15% stretching. Beyond this pressure, the corneal gel became denatured or physically damaged to prevent its complete recovery. Excessive IOP also induced a phase transition in the whole eye. That is, the in situ cornea became opaque when the IOP of the calf eye under normal conditions (~9–21 mmHg) was increased by ~35 mmHg. The opacity

was reversed when the excessive IOP was removed. Hence the overall data presented herein are suggestive of the hypothesis that corneal opacity induced by excessive IOP may well be due to a phase transition.

For the case where a gel undergoes a phase transition induced by increased temperatures, polymer-polymer interactions become predominant as the entropy of water increases. Hence gels that collapse upon increased temperatures are considered to be hydrophobic (Hirotsu et al. 1987). Although glycosaminoglycans are hydrophilic polymers, the behavior of the collagen gel matrix parallels hydrophobic gels and the cornea is thus considered to be a "hydrophobic" gel.

It had long been predicted theoretically that compressing or stretching a gel could induce phase transitions. This study presents new experimental evidence for a gel undergoing a phase transition upon stretching. That the cornea undergoes a phase transition upon stretching is unique. This simple observation may be helpful towards the understanding of reversible processes in opacity observed when the cornea is subjected to conditions of excessive intraocular pressures, as in acute glaucoma. The study also indicates that reversible corneal opacities observed after laser ablation may well be due to a temperature induced phase transition. To develop a more thorough understanding of the corneal dynamics under external stresses, however, much more conclusive investigations of the cornea using microscope laser light scattering are warranted, which is the subject of future studies.

In conclusion, microscope laser light scattering spectroscopy can be used as an effective tool for determining essential physical characteristics of the cornea, in particular, the corneal stroma. The corneal stroma is a complex gel matrix that most likely exhibited critical behavior upon increased temperatures, thereby indicating that it is a hydrophobic gel. Critical behavior was also observed upon increased corneal stretching and intraocular pressures. Hence, it is hypothesized that primary corneal opacity is due essentially to reversible critical density fluctuations associated with phase transitions of the corneal gel upon increased temperatures or stretching. The critical density fluctuations most probably correspond to the formation of fibril "lakes." Moreover, the study also exhibited preliminary evidence suggesting that lamellar layers within the stroma can be considered as individual gel sheets. This study not only makes use of dynamic light scattering techniques to investigate the cornea, but also invokes phase transition and critical behavior of gels as a probable means to describe the physical characteristics of the cornea. The possible application of the dynamic light scattering and polymer theories in the clinical investigations of the cornea merits the considerable efforts required to develop a more thorough physical-chemical understanding of corneal opacities.

Acknowledgements This work was supported by NIH, EY05272-05. The George R. Harrison Spectroscopy Laboratory was supported by NIH, P41-RR02594. The authors thank Dr. M. Tokita and Dr. W. M. Zuk for valuable discussions and suggestions.

References

Amiya T, Tanaka T (1987) Phase transitions in cross-linked gels of natural polymers. Macromolecules 20:1162–1164

Benedek GB (1971) Theory of transparency of the eye. Appl Optics 10:459–473

Berne BJ, Pecora R (1976) Dynamic light scattering. Plenum Press, New York

Bettelheim FA, Vinciguerra MJ (1969) Low-angle laser scattering of bovine cornea. Biochim Biophys Acta 177:259–264

Cejtlin J, Vinciguerra MJ, Bettelheim FA (1971) Changes in the molecular superstructure of bovine cornea under stress. Biochim Biophys Acta 237:530–536

Farrell RA, McCally RL (1976) On corneal transparency and its loss with swelling. J Opt Soc Am 66:342–345

Feuk T (1970) On the transparency of the stroma in the mammalian cornea. IEEE Trans Biomed Eng 17:186–190

Flory PJ (1953) Principles of polymer chemistry. Cornell University Press, Ithaca

de Gennes PG (1979) Scaling concepts in polymer physics. Cornell University Press, Ithaca, pp 214–216

Gisselberg M, Clark JI, Vaezy S, Osgood TB (1991) Evaluation of Fourier components in cornea. Am J Anat 191:408–418

Hecht AM, Geissler E (1980) Gel deswelling under reverse osmosis. J Chem Phys 73:4077

Hirotsu S, Hirokawa Y, Tanaka T (1987) Volume-phase transitions of ionized N-isopropylacrylamide gels. J Chem Phys 87:1932

Kikkawa Y (1960) Light scattering studies of the rabbit cornea. J Physiol Soc Jpn 10:292–302

Landau LD, Lifshitz EM (1980) Lifshitz EM, Pitaevskii LP (eds) Statistical physics, 3rd edn, part 1. Pergamon, Oxford, pp 483–488

Lange's Handbook of Chemistry (1985) Dean JA (ed), 13th edn. McGraw-Hill, New York, pp 10–96

Li Y (1989) Structure and critical behavior of polymer gels. PhD Thesis, Massachusetts Institute of Technology

Lohmann CP, Timberlake GT, Fitzke FW, Gartry DS, Kerr-Muir M, Marshall J (1992) Corneal light scattering after excimer laser photorefractive keratectomy: the objective measurements of haze. Refract Corneal Surg 8:114–121

Mamada A, Tanaka T, Kungwatchakun D, Irie M (1990) Photoinduced phase transition of gels. Macromolecules 23:1517–1519

Maurice DM (1984) The cornea and sclera. In: Davson H (ed) The Eye, 3rd edn. Academic Press, New York, pp 1–158

McCally RL, Farrell RA (1977) Effect of transcorneal pressure on small angle light scattering from rabbit cornea. Polymer 18:444–448

Meek KM, Fullwood NJ, Cooke PH, Elliot GF, Maurice DM, Quantock AJ, Wall RS, Worthington CR (1991) Synchrotron x-ray diffraction studies of the cornea, with implications for stromal hydration. Biophys J 60:467-474

Nishio I, Tanaka T, Sun ST, Imanishi Y, Ohnishi ST (1983) Hemoglobin aggregation in single red blood cells of sickle cell anemia. Science 220:1173–1175

Peetermans J, Nishio I, Ohnishi ST, Tanaka T (1986) Light scattering study of depolymerization kinetics of sickle hemoglobin polymers inside erythrocytes. Proc Natl Acad Sci USA 83:352–356

Scott JE, Haigh M (1985) "Small"-proteoglycan:collagen interaction: keratan sulfate proteoglycan associates with rabbit corneal collagen fibrils at the "a" and "c" bands. Biosci Rep 5:765–771

Tanaka T (1978) Dynamics of critical concentration fluctuations in gels. Phys Rev A 17:763–766

Tanaka T, Fillmore DJ (1979) Kinetics of swelling gels. J Chem Phys 70:1214–1218

Tanaka T, Hocker LO, Benedek GB (1973) Spectrum of light scattered from a viscoelastic gel. J Chem Phys 59:5151–5159

Tanaka T, Sun ST, Nishio I (1980) Phase transitions in gels. In: Chen SH, Chu B, Nossal R (eds) NATO Adv Study Inst Ser, Ser B, vol 73. Plenum Press, pp 321–336

Waltman SR, Hart WM (1970) The cornea. In: Moses RA (ed) Adler's physiology of the eye; clinical application. Mosby, St. Louis, pp 36–59